

Article

GPR and ERT Investigations in Urban Areas: The Case-Study of Matera (Southern Italy)

Jessica Bellanova ¹, Giuseppe Calamita ¹ , Iliara Catapano ² , Alessandro Ciucci ³, Carmela Cornacchia ¹, Gianluca Gennarelli ², Alessandro Giocoli ⁴, Federico Fisangher ³, Giovanni Ludeno ² , Gianfranco Morelli ³, Angela Perrone ¹, Sabatino Piscitelli ¹, Francesco Soldovieri ²  and Vincenzo Lapenna ^{1,*}

- ¹ Istituto di Metodologie per l'Analisi Ambientale, CNR, C.da S.Loja, I-85050 Tito (PZ), Italy; jessica.bellanova@imaa.cnr.it (J.B.); giuseppe.calamita@imaa.cnr.it (G.C.); carmela.cornacchia@imaa.cnr.it (C.C.); angela.perrone@imaa.cnr.it (A.P.); sabatino.piscitelli@imaa.cnr.it (S.P.)
 - ² Istituto per il Rilevamento Elettromagnetico dell'Ambiente, CNR, Via Diocleziano 328, I-80124 Naples, Italy; catapano.i@irea.cnr.it (I.C.); gennarelli.g@irea.cnr.it (G.G.); ludeno.g@irea.cnr.it (G.L.); soldovieri.f@irea.cnr.it (F.S.)
 - ³ Geostudi Astier S.r.l., Via Edda Fagni 31, I-57123 Livorno, Italy; ciucci@geostudiastier.com (A.C.); fisangher@geostudiastier.com (F.F.); morelli@geostudiastier.com (G.M.)
 - ⁴ Centro Ricerche Trisaia, ENEA, S.S. 106 Ionica, km 419+500, I-75026 Rotondella (MT), Italy; alessandro.giocoli@enea.it
- * Correspondence: vincenzo.lapenna@imaa.cnr.it

Received: 20 April 2020; Accepted: 4 June 2020; Published: 10 June 2020



Abstract: This paper deals with a geophysical survey carried out in some critical urban areas of the historical city of Matera (Southern Italy). Matera has a very complex shallower stratigraphy characterized by both anthropic and natural “targets” and is affected by geological instability. Therefore, Matera represents an ideal and very challenging outdoor laboratory for testing novel approaches for near-surface explorations in urban areas. Here, we present the results of a near-surface survey carried out by jointly applying Ground Penetrating Radar (GPR) and Electrical Resistivity Tomography (ERT) methods. The survey was implemented in three different critical zones within the urban area of Matera (Piazza Duomo, Piazza San Giovanni, Villa dell’Unità d’Italia). These test sites are of great interest for archaeological and architectural studies and are affected by ground instability phenomena due to the presence of voids, cavities and other anthropic structures. The effectiveness of the survey was enhanced by the exploitation of advanced 3D tomographic approaches, which allowed to achieve 3D representation of the investigated underground and obtain information in terms of both the location and the geometry of buried objects and structures and the characterization of shallow geological layers. The results of the surveys are now under study (or have attracted the interest) of the Municipality in order to support smart cities programs and activities for a better management of the underground space.

Keywords: near-surface geophysics; electromagnetic sensing; 2D and 3D tomography; smart and resilient cities

1. Introduction

Today, there is an increasing awareness about the necessity of smart management and protection of the urban areas, which is one of the main elements ensuring the Smart City paradigm. The latter one considers the good and reliable behaviour of the urban areas as strictly affected by the functioning of the service networks interacting one to each other and mutually dependent. In fact, a Smart City can behave in a reliable way only when the good functioning of the critical infrastructures/services, such as

energy, ICT, mobility and so on, is ensured. Therefore, the concept of smartness is strongly linked to resilience, which has to be ensured during ordinary situations and crisis events [1–3].

The risk scenarios of urban areas and of their infrastructures are the result of the combination of their vulnerability (dictated by their condition and resilience capabilities) with the hazards due to the different environmental and anthropic causes. In this frame, it is worth underlying that urban areas, when characterized by a degraded condition, could be damaged seriously even by events whose impact would be negligible in “normal situations”. These considerations bring the necessity to carry out a long-term monitoring and assessment of the status of cities and of the embedded infrastructures in view of enabling “risk-scenario analysis” tools [4–6].

In this general context, it is crucial to ensure the monitoring and the management of the underground environment, which has to be seen not only in terms of the mitigation of risks factors but even as the search for and exploitation of resources generating economic, social and cultural value [7–9]. Indeed, the shallower layers of the subsoil represent the “reservoir” of economic and cultural resources (structures and foundations, archaeological assets, subservices: pipes, cable ducts, networks, etc.) and the “physical space” in which to build strategic underground infrastructures (networks energy, networks for urban mobility, sub-services of the aqueduct, etc.). This dual aspect also entails the necessity to plan the actions impacting the underground on the basis of a trade-off between different needs. As an example, the underground environment of the urban area is often a “cultural heritage asset”, where buried archaeological remains can be a factor of social and economic growth. At the same time, the archaeological remains also represent an “obstacle” for the execution of the urban management activities, because their preservation entails stringent constraints about the planning and execution of engineering works.

Accordingly, one of the main scientific and technological challenges is the development and the cooperative application of non-invasive diagnostic methodologies in order to obtain 2D and 3D high-resolution imaging of the urban subsoil [10]. The combination ensures the overcoming of applicability drawbacks of a single methodology in urban area and allows the achievement of useful information on the subsurface at different depths and with different spatial resolutions.

Here, we present the first results of a geophysical survey carried out in several critical urban areas of the historical city of Matera (Basilicata Region, Southern Italy), potentially affected by hydrogeological instability phenomena. The research activities were planned and carried out under the frame of the CLARA Smart Cities project “CLoud pLAtform and smart underground imaging for natural Risk Assessment in urban areas” and was funded by the Italian Ministry of Education, University and Research (MIUR). Matera was designated European Capital of Culture in 2019 and its historical center of the Sassi is recognized as an UNESCO World Heritage Site. According to the UNESCO declaration “Matera is the most outstanding, intact example of troglodyte settlement in the Mediterranean region, perfectly adapted to its terrain and ecosystem. The first inhabited zone dates from the Paleolithic, while later settlements illustrate a number of significant stages in human history”. The urban area of Matera is characterized by an underground scenario that is very rich in terms of the presence of environmental features such as cavities, voids and anthropic structures related to pre-existing urban assets [11]; this is also due to the particular nature of the material in the shallower underground.

In this paper, we focus on geophysical surveys carried out at three of the most interesting and fascinating squares of the historical center of Matera, which are “Piazza Duomo”, “Piazza S. Giovanni” and “Villa dell’Unità di Italia” (Figure 1). These sites are important for their presence in the same area of cavities, tanks and archaeological remains. The underground investigation in Matera was specifically carried out in order to identify and characterize the presence of cavities, but even to detect areas affected by micro-subsidence and hydrogeological risks.



Figure 1. Map of the historical center of the “Sassi di Matera” that since 1993 is in the list of UNESCO World Heritage Sites with the location of the three test sites. (Image modified from Google Earth).

Herein, we present the results of a geophysical approach based on the joint application of Ground Penetrating Radar (GPR) and Electrical Resistivity Tomography (ERT) methods for the 2D and 3D imaging of the underground space. GPR surveys were applied for exploring the shallower layers of the subsurface with very high resolution (tens of centimeters), mostly for the detection and geometric characterization of buried ancient structures. Furthermore, GPR surveys were crucial for characterizing the presence of anthropic elements, such as subservices pipes and metallic reinforcement structures. The ERT method allowed to extend the investigation depth up to a few tens of meters and it was deployed to gain information not only about large anthropic elements, but more importantly, about the lithological-structural elements of the underground, with a resolution of a few meters.

The results consisting of 2D and 3D subsurface images allowed the reconstruction of the subsoil geological setting and the identification of buried cavities and archaeological remains. The results have highlighted the potentiality of the proposed approach that can be considered a useful tool to support the planning of possible maintenance interventions respecting the social and cultural value of the investigated site.

2. Materials and Methods

2.1. The Test Site

The city of Matera is located in the Basilicata Region, Southern Italy. Since 1993, it has been defined as a World Heritage Site by UNESCO thanks to the presence of the “Sassi” historical center and the “Park of the Rupestrian Churches”, which are prehistoric settlements comprising houses, churches, monasteries and hermitages built into the natural caves of the Murgia. Due to its richness of cultural heritage and historical values, Matera was designated the European Capital of Culture in 2019 [12].

From a geological perspective, the territory of the urban area of Matera falls within a geological-structural transition context between the Apulian Foreland and Bradanic trough. The city of Matera arises at the eastern edge of the Bradanic trough, a large depression set in the Middle Pliocene in the Mesozoic substrate formed by Altamura Limestones and characterized by the presence of two structural highs, one in the south-west area of the city, called Horst di Zagarella [13,14] and the other to the south-east, called Horst of Matera (Figure 2). On the calcareous substrate, calcarenitic deposits (Calcarenites of Gravina) have settled and in succession, there are fine clastic materials represented by Pleistocene marine clays. Superimposed on the latter ones, sandy and terraced conglomeratic

deposits are found as closure of the Pliocene-Pleistocene sedimentary cycle. The morphology of the territory, characterized by deep gorges (gravine) and bare highland plateaus, integrated with ancient cave churches, shepherd tracks marked by wells and fortified farmhouses, forms one of the most evocative landscapes of the Mediterranean area [15].

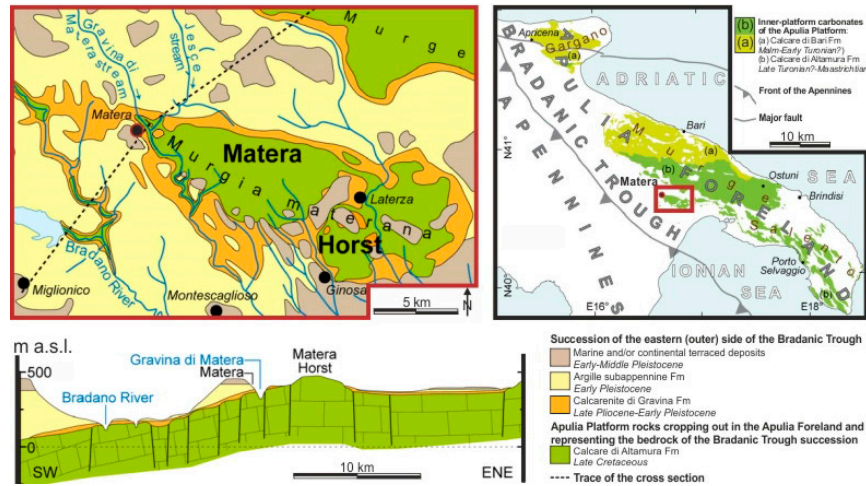


Figure 2. Geological setting of the surrounding area of the urban area of Matera (modified from Festa et al. 2018).

The geophysical survey was carried out at three different test sites representing the most important squares of the city. The first area under investigation is Piazza Duomo and is located close to the ancient district of the Sassi, where calcarenitic deposits crop out, reaching thicknesses of about 40 m. In particular, Piazza Duomo is located on the highest spur of the Civita, considered the oldest part of the Matera town located between the Sasso Barisano and the Sasso Caveoso. The cathedral of Madonna della Bruna and Sant'Eustachio, built in the Apulian Romanesque style in the 13th century, stands in the square and represents the main place of Catholic worship in the city of Matera, the mother church of the archdiocese of Matera-Irsina. This area has an enormous historical and architectural significance and represents an extraordinary factor of tourist attraction.

The second area under investigation, Piazza San Giovanni, is located outside the walls of the ancient city. The square under study houses the Church of San Giovanni Battista, a cult building dating back to medieval times and considered an architectural jewel due to its refined architectural composition and fine decoration. This monument has an enormous historical and architectural value that represents an extraordinary factor of tourist attraction and that, as such, must be preserved and handed over to future generations. Considering the historical and architectural significance of both squares, as well as the role they play for tourism in the city, an in-depth study of the subsoil, focusing on the identification of cavities and hypogeum and on the delimitation of potential areas affected by instability phenomena, assumes a strategic importance.

The third area interested by the geophysical investigations is Villa dell'Unità d'Italia. This square is located in the modern area of the city where silty-clayey soils, belonging to the alluvial deposits and the formation of Sub-Apennine Clays overlay calcarenitic deposits. The Villa occupies a triangular area of about 3.850 m², oriented with the vertices to the north-west, south-east and south-west, generated by the intersection of three road axes. It was built around the 1930s, to make up for the old abandoned botanical garden for the construction of the Palazzo della Provincia, at the intersection of Via D. Ridola and Via Lucana. The Villa presents various monumental works and is a space for citizenship social aggregation. For these reasons, the geophysical investigations were planned for mapping the water saturated zones potentially responsible for micro subsidence and for investigating the geometrical boundaries between the silty-clayey layers and the calcarenite materials.

2.2. Ground Penetrating Radar

One of the key sensing technologies usually deployed for underground prospecting is Ground Penetrating Radar (GPR), which is commonly used for high-resolution diagnostics of the shallower layers of the underground (till a few meters). GPR is a “friendly” technology only when applied in very simple cases. Indeed, when complex scenarios (such as the ones arising in underground inspection) are faced, the interpretability of GPR data is rather challenging and it is necessary to perform an advanced data processing [16]. One of the most used data processing techniques is Microwave Tomography (MT) that states that GPR imaging is the more general framework of an electromagnetic inverse problem. For this inverse problem, one aims at achieving the detection, localization and geometry estimation of hidden targets starting from the backscattered field collected by probing the scenario under test by means of a known incident field [17].

The effectiveness of the GPR survey in Matera was not only enhanced by using MT but also thanks to the deployment of a prototype GPR system, namely the IDS Stream-X (Subsurface Tomographic Radar Equipment for Assets Mapping) equipped with a 16 channel 200 MHz array, which works at the single nominal frequency of 200 MHz.

As usual in surface penetrating radar, a reflection configuration is adopted and the offset between the transmitting and receiving antennas is negligible in terms of the probing wavelength. Accordingly, a monostatic measurement configuration is adopted. The peculiarity of the system is its capability of collecting simultaneously 16 radargrams (or B-scans) evenly spaced at 12 cm, so that, for each radar passage, a swathe of 1.80 m is investigated. The dimension of the antenna system is 2.4 m × 0.92 m and the weight is about 36 kg. The system can collect data by moving at a speed of 15 km/h.

At Matera each B-scan has been acquired by fixing a spatial offset of 0.017 m between two consecutive A-scans (radar traces); for each A-scan, the acquisition time window was set equal to 127 ns (fast time) and discretized by means of 512 samples. To achieve a complete coverage of the survey area, multiple passes are controlled through sophisticated positioning systems and a dedicated navigation software.

GPR results were obtained by means of a microwave tomographic approach specifically tailored for the Stream-X system and able to provide 3D images of the underground under the form of constant depth slices. More in detail, the data were elaborated by using a dedicated data processing strategy made by three main key phases: (i) pre-processing; (ii) data inversion; (iii) pseudo 3D representation of the scene.

Pre-processing is a sequence of standard time-domain (TD) procedures, which aim at extracting the useful signal from raw data by removing direct antenna coupling, reducing noise and emphasizing the presence of the target. It begins with the zero-timing correction and involves procedures, such as time gating (TG) and background (BKG) removal, which help to remove or mitigate the signal contributions due to the antenna coupling, the air-material interface and (undesired) horizontal reflectors [18,19]. Herein, the zero-timing is used to cut the first part of the signal, up to the reflection of the air-medium interface, which is hypothesized to be flat.

In this way, the zero-time of the B-scan is fixed in correspondence of the air-medium interface and, accordingly, B-scan accounts only for the signal propagation and scattering inside the probed underground. The TG procedure is used to erase the signal due to the direct antenna coupling and to select the portion of the observation time window wherein the useful signal is expected to occur. The BKG removal procedure is applied to reduce the signal portion due to the interfaces present in the data and usually provides a cleaner image of buried targets, but for extended flat material interfaces.

Data inversion, instead, performs target reconstruction and exploits microwave tomography to face the imaging problem. In particular, the imaging problem is formulated into the frequency domain by considering a homogeneous 2D scalar model of the underlying scattering phenomenon. The inverse scattering problem is tackled by exploiting the Born approximation in order to define the mathematical relationship describing the interactions between microwaves and electromagnetic features of the investigated scenario [20].

Finally, pseudo 3D representation merges the 2D microwave tomographic images provided by the data inversion in order to obtain a 3D representation of the investigated areas and the results are presented as constant-depth slices.

Coming back to the data inversion procedure, it processes a single GPR profile (B-Scan) by assuming as a reference scenario a 2D homogeneous, non-dispersive, and non-magnetic medium characterized by a constant relative dielectric permittivity, ϵ_b . The scattering phenomenon is activated by means of antennas, which are modelled as filamentary sources polarized along the invariance axis and fed by a unitary current. The transmitting and receiving antennas are located at the air-medium interface and their horizontal offset is negligible. Hence, the scattering model is defined under a multi-monostatic/multi-frequency reflection measurement configuration.

Let Ω be the probed domain, i.e., the spatial region where the targets to be imaged are located, r the generic point in Ω and $\chi(r) = \frac{\epsilon(r)}{\epsilon_b} - 1$ the contrast function accounting for the variations of the equivalent permittivity with respect to that of the investigated medium. According to these assumptions, the scattering phenomenon is described, at each angular frequency, by a linear integral equation [20]:

$$E_s(x_s, x_0, \omega) = k_b^2 \int_{\Omega} G(x_0, \omega, r) E_{inc}(x_s, \omega, r) \chi(r) dr \quad (1)$$

where E_s denotes the scattered field measured in x_0 when the probing source is at $x_s = x_0$, E_{inc} is the incident field in Ω , i.e., the field into the probed region in the absence of any target, k_b is the wave number into the background medium and G is the known Green's function referred to the scenario at hand.

The integral equation (Equation (1)) is discretized according to the Method of Moments by using a pixel based representation for the unknown contrast function. Accordingly, the imaging is faced as the solution to the following matrix problem:

$$E_s = L[\chi] \quad (2)$$

In Equation (2), E_s is the $K = M \times F$ dimensional data vector, M being the number of spatial measurement points and F the number of frequencies, χ is the N -dimensional unknown vector, N being the number of points in Ω ; L is the $K \times N$ dimensional matrix obtained by discretizing Equation (1). It is worth noting that the matrix L depends on the adopted measurement configuration as well as on the reference scenario.

Accordingly, the position of the measurement points as well as the electromagnetic parameters of the probed medium need to be known to define L , properly. Moreover, due to the fact that the linear system in Equation (2) derives from the discretization of an ill-posed integral equation, its solution, i.e., the inversion of the matrix L , is an ill-conditioning problem [21]. Hence, its solution is very sensitive to measurement uncertainties and noise in the data. In order to obtain a stable approximate solution, a regularization scheme has to be applied and the Truncated Singular Value Decomposition (TSVD) scheme [21] is herein adopted. Accordingly, an approximated solution of Equation (2) is given by:

$$\tilde{\chi} = \sum_{n=1}^H \frac{\langle E_s, u_n \rangle}{\sigma_n} v_n \quad (3)$$

where \langle, \rangle denotes the scalar product in the data space, H is the truncation index, $\{\sigma_n\}_{n=1}^Q$ is the set of singular values of the matrix L ordered in a decreasing way, $\{u_n\}_{n=1}^Q$ and $\{v_n\}_{n=1}^K$ are the sets of the singular vectors in the data and unknown spaces, respectively. The threshold $H \leq Q$ ($Q = \min\{K, N\}$) defines the "degree of regularization" of the solution and is chosen as a trade-off between the accuracy and resolution requirements from one side (which suggest a larger H value) and solution stability from the other side (which is required to keep a low H). The imaging result is given as the spatial map of the modulus of the retrieved contrast vector $\tilde{\chi}$ normalized to its maximum value in the scene. Hence,

the regions of Ω where the modulus of $\tilde{\chi}$ are significantly different from zero indicate the position and geometry of the targets [19,20].

2.3. Electrical Resistivity Tomography

To date, the Electrical Resistivity Tomography (ERT) represents a robust geophysical method for the near-surface investigations. It is applied in a wide spectrum of geological, environmental and engineering problems [22–25]. A DC electrical current is injected in the subsoil using an energising multi-electrode system deployed along a profile and the generated voltage signals are detected on the surface with a receiving electrode system. Many different electrode layouts can be used, however, dipole-dipole, Schlumberger and Wenner configurations are the most common ones. Taking into account the geometry of the electrode systems, from the analysis of the voltage signals it is possible to obtain 2D or 3D electrical pseudo-section, in which the spatial distribution of the apparent resistivity is represented. Finally, by means of algorithms performing the data inversion it is possible to obtain an electrical resistivity tomographic map.

At Matera, the geoelectrical surveys were performed with a Syscal Pro Switch 96 (Iris Instruments) equipped with a transmitter capable of delivering currents up to 2.5 A and by applying voltages up to 800 V (250 W). The tool allows the simultaneous management of a maximum number of 96 electrodes, automatic execution of the measurement sequence and the compensation of the spontaneous potential. Considering the logistic conditions (size of the square and passage of pedestrians and cars during the acquisition), it was not possible to use a very dense acquisition grid. The electrodes used at the same time were 2 m apart. The acquisition with dipole-dipole and pole-dipole devices, with transmitter (TX) and receiver (RX) diffused over the whole grid, allowed us to compensate for the lack of sensitivity due to the basic electrode step and to avoid strong local effects. The geoelectric data were subsequently processed and inverted with the ERT Lab software, developed by Geostudi Astier, which uses a finite-element (FEM) approach to model the subsoil. Throughout the inversion iterations, the effect of non-Gaussian noise was appropriately managed using a robust data weighting algorithm [26,27].

3. Results

This section aims to describe the results obtained by processing GPR and ERT data acquired during the survey carried out in Matera by means of the strategies described in Section 2. In particular, Piazza Duomo was investigated by using both GPR and ERT methods, whereas on Piazza San Giovanni and Villa dell'Unità d'Italia only GPR and ERT were used, respectively.

As far as the GPR data is concerned, the raw data, collected in both test sites, were processed by using the same filtering parameters. Specifically, the zero time of the radargram was set at 7 ns and the time gating procedure was also applied in order to select the signal portion between 12 ns and 57 ns. By doing so, the direct coupling between the antennas, which completely overwhelms the backscattered signal due to buried targets, is erased; in addition, the signal portion after 57 ns, which is characterized only by noise, is filtered out. As a consequence, by assuming that the surveyed medium is characterized by a relative permittivity whose average value is equal to $\epsilon_b = 9$, the maximum investigation depth is $z = 2.50$ m. After, the fast Fourier transform was performed to obtain the frequency domain data needed as input to the data inversion. In this frame, the effective frequency range of the data was estimated by means of a spectral analysis and it ranged from 100 MHz up to 600 MHz and was sampled by 26 evenly spaced frequencies. All the presented results have been obtained by setting the TSVD threshold in such a way to filter out all the singular values that are 25 dB lower than the maximum one.

3.1. Piazza Duomo

The GPR and ERT surveys carried out on Piazza Duomo were planned in order to obtain information on the possible presence of buried structures, as cisterns for water storage and ducts. The area has a surface of approximately 534 m², whose length is 13.45 m along the North direction (later referred as x-axis) and 39.80 m along the East direction (later referred as y-axis) in Figure 3.

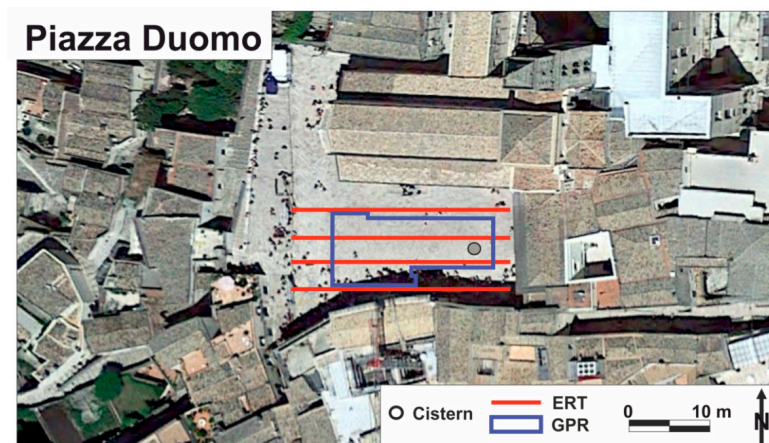


Figure 3. Limits of the investigated area within the “Piazza Duomo”, survey lines and location of the old cistern (Image modified from Google Earth).

In order to achieve its complete coverage, 8 GPR passages were carried out by means of the Stream-X, hence 120 B-scans were gathered after being processed according to the tomographic approach described in Section 2.2. Figure 4a–f show the depth slices of the investigated area obtained by cutting the 3D reconstruction at the depths $z = 0.15$ m, $z = 0.69$ m, $z = 0.96$ m, $z = 0.99$ m, $z = 1.23$ m, $z = 1.50$ m, $z = 1.77$ m. These images reveal the presence of several buried structures used to direct and store the water. Specifically, the structures having an elongated shape may be ascribed to ducts, while those of circular and rectangular shape could represent the cisterns. An interpretation of the most representative depth slices is given in Figure 5, where the dashed white lines depict the recognized structures. In particular, the manhole visible on the stone pavement of Piazza Duomo (see Figure 3) is clearly visible in the tomographic image at $z = 0.15$ (see Figure 5a); while a circular cistern, whose diameter is about 10 m, begins at $z = 0.69$ m (see Figure 5b). The water was directed into this circular cistern by means of an oblique duct, which starts to appear at $z = 0.69$ m and it is reconstructed completely in the image at depth $z = 0.96$ m (see Figure 5c). This phenomenon is due to the slope given to the duct in order to conduct the water into the cistern. In Figure 5c, two further ducts are visible. One is on the left side of the image and is about 10 m long; while a small duct appears around $y = 16$ m and it is connected with the duct going towards the circular cistern.

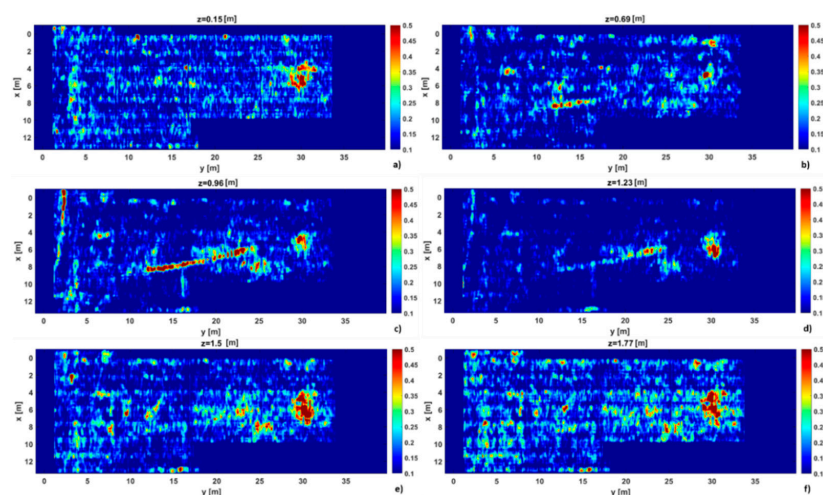


Figure 4. Visualization of the pseudo-3D GPR tomographic results by means of slices at different depths: (a) 0.15 m; (b) 0.69 m; (c) 0.96 m; (d) 1.23 m; (e) 1.5 m; (f) 1.77 m. Several anomalies are visible, which are ascribed to the presence of duct and cisterns for water storage. The tomographic images show the normalized intensity of the obtained contrast.

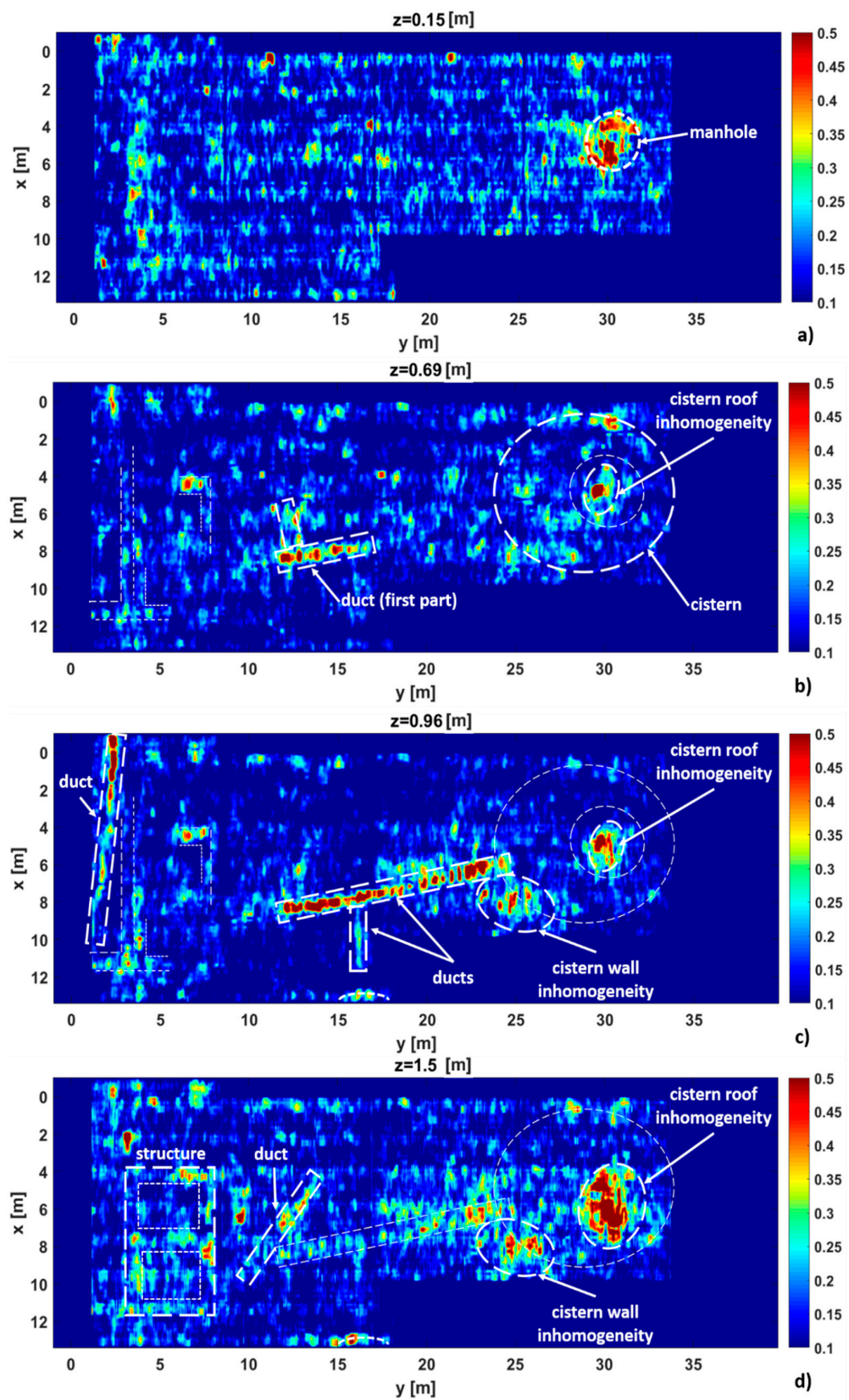


Figure 5. Interpretation of the pseudo-3D GPR tomographic results GPR tomographic results. Specifically, the images at the most significant depths are provided: (a) 0.15 m; (b) 0.69 m; (c) 0.96 m; (d) 1.5 m. The detected structures are represented by means of dashed white lines and identified.

Moreover, the image at depth $z = 1.5$ m (see Figure 5d) reveals the presence of a rectangular shaped structure, which seems to be made up by two rooms and start to appear at shallower depths. This structure is connected with the duct appearing completely on the left side of the image at $z = 0.96$ m. In Figure 5d, another oblique duct appears and seems to be connected with the rectangular structure and the duct going towards the circular cistern. Finally, two further anomalies are localized in the area of the circular cistern and they could be related to some inhomogeneity of the roof and a portion of the perimeter wall of the cistern. In order to clarify how these anomalies are located in the cistern area, the manhole representation was repeated in Figure 5b,c.

In order to investigate the deeper layers of the subsurface, an ERT survey was carried out using a Syscal Pro Swich 96 with 96 electrodes regularly distributed on the surface. To avoid logistic problems and local effects, we used the dipole-dipole and pole-dipole configurations with a distance between the electrodes of 2 m. The 3D ERT model obtained using the ERT Lab software reached a maximum depth of 8 m (see Figure 6a). The resistivity pattern highlighted the stratigraphic boundary between the resistive zone ($\rho > 300 \Omega\text{m}$) related to the Calcarenite di Gravina with the more superficial conductive material ($\rho < 300 \Omega\text{m}$) that could be attributed to the anthropogenic infill. The low resistivity values of the shallower layers might be due to the lithological nature (e.g., clays, silt) or to unconsolidated material with a higher water content. The contact between the conductive shallower (surface) material and the resistive one placed deeper is clearly visible in the 2D vertical section of electrical resistivity (see Figure 6b) crossing the center of the square. The representation of the resistivity values with horizontal slices at increasing depths (see Figure 7) allows the localization of the cistern, positioned in the first 3 m of subsurface in the western zone of the square. Finally, the sharp transition from conductive to resistive material is clearly visible at the depth of 5 m

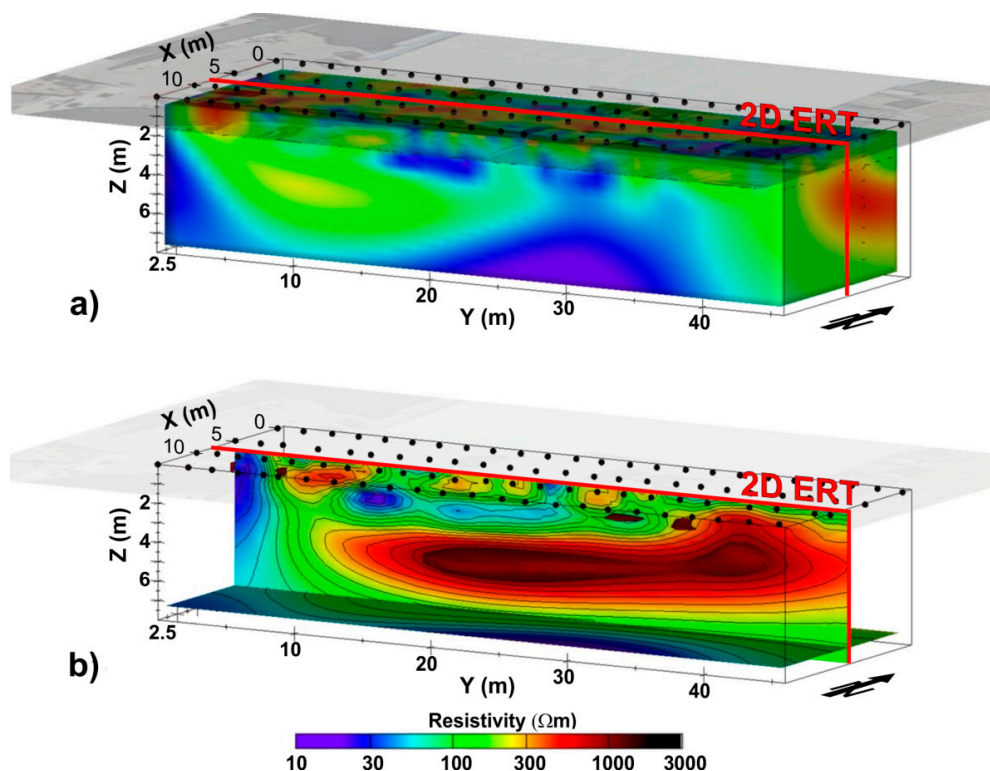


Figure 6. (a) 3D ERT model obtained at the investigated area of “Piazza Duomo”; (b) a 2D ERT section relative to the geoelectrical measurements obtained in the central part of “Piazza Duomo”, the high resistive zone is related to the presence of a subsurface cistern.

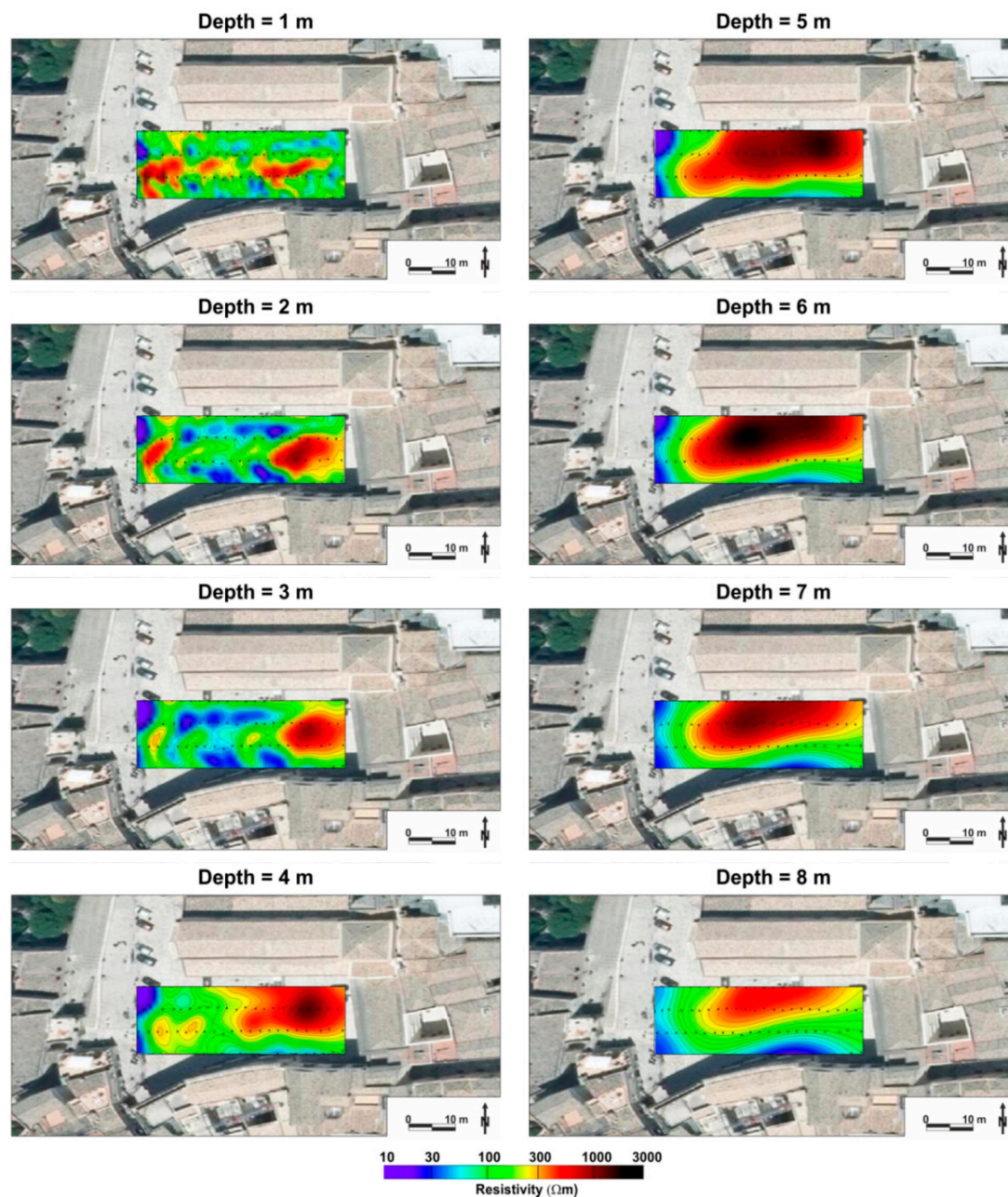


Figure 7. Results of the 3D ERT tomographic images represented by means of constant depth slices (Image modified from Google Earth).

3.2. Piazza San Giovanni

The geophysical survey at San Giovanni square was planned to investigate an area of 586 m^2 , whose lateral extensions were 35 m and 18 m respectively (see Figure 8a). The investigated area was close to the San Giovanni Battista church and its portion covered an area that was the matter of an archaeological survey, which allowed the discovery of tombs and ancient walls (see Figure 8b,c) [28]. The entrance of the San Giovanni Battista church corresponds to the position ($x = 0\text{ m}$; $y = 7\text{ m}$) on the tomographic images.

The GPR Stream-X measurements were performed along 17 profiles and 255 B-scans were collected, covering the area depicted in Figure 8. In Figure 9a–d the main results obtained from the processing of the GPR data are displayed by using slices at depths: $z = 0.18\text{ m}$, $z = 0.24\text{ m}$, $z = 0.30\text{ m}$ and $z = 0.87\text{ m}$.

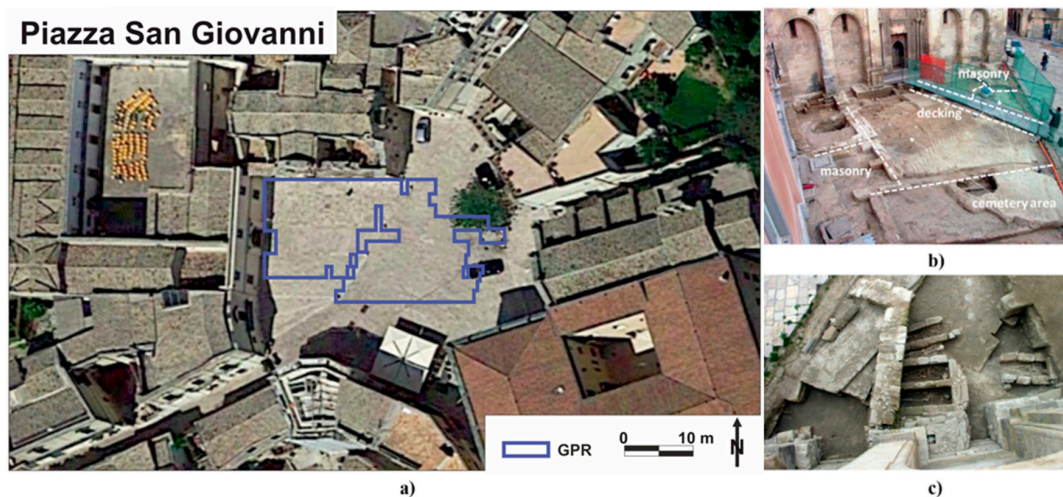


Figure 8. (a) Map of the investigated area at Piazza San Giovanni. (Image modified from Google Earth). (b,c) tombs and walls discovered during an archaeological survey carried out in the past years.

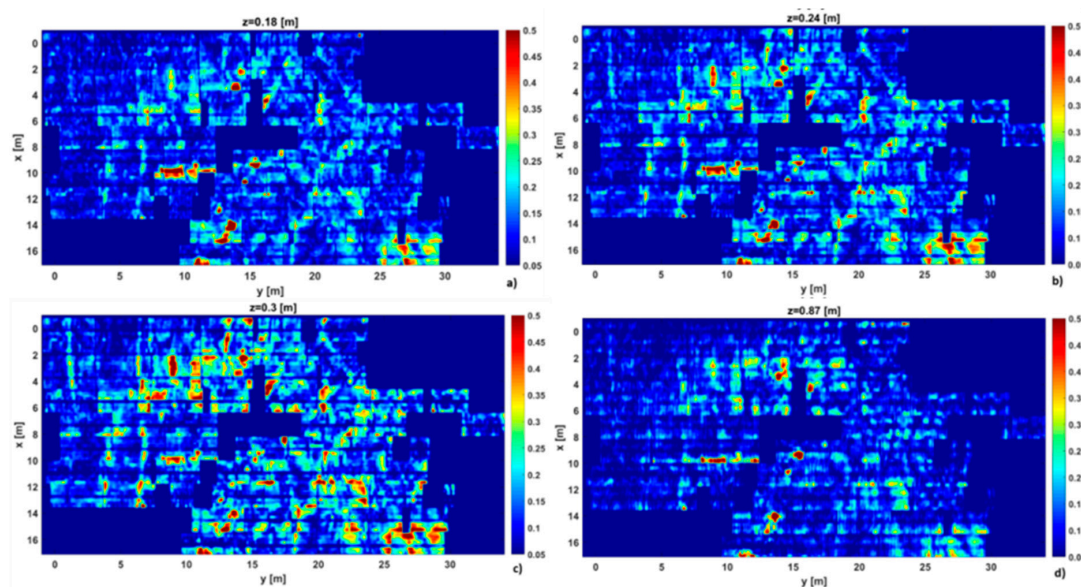


Figure 9. Visualization of the pseudo-3D GPR tomographic model by means of constant slices at different depths: (a) 0.18 m, (b) 0.24 m; (c) 0.3 m; (d) 0.87 m. The tomographic images show the normalized intensity of the obtained contrast.

The tomographic reconstruction at depth $z = 0.18$ m shows the degree of anthropization of the shallow part of the subsurface, while several scatterers, widespread in the investigated area, appear at a depth of $z = 0.24$ m and $z = 0.3$ m. An interpretation of the tomographic image at $z = 0.3$ m is given in Figure 10a, where the white dashed lines represent the detected masonry structures. Such an interpretation was limited to the cemetery area, which was retrieved in front of the church during an archaeological survey carried out in the past years [28]. In Figure 10a, the hypogeum is also denoted in the down right corner, at y ranging from about 25 m to 30 m. Finally, a square shaped structure covering an area of about 16 m^2 appears at depth $z = 0.87$ m (see Figure 10b).

The high level of the anthropization, the presence of the wire meshes and the poor electrode ground contacts made the processing of the ERT images impossible and unreliable. In fact, the geoelectric data acquired in Piazza San Giovanni were particularly noisy and proved to be dominated by the effects produced by the interventions carried out during 2007 for the refurbishment of the

pavement and the rearrangement of the underground structures [28,29]. Then, by taking into account the GPR results and the first field tests for the resistivity measurements, the ERT survey was not carried out in this area.

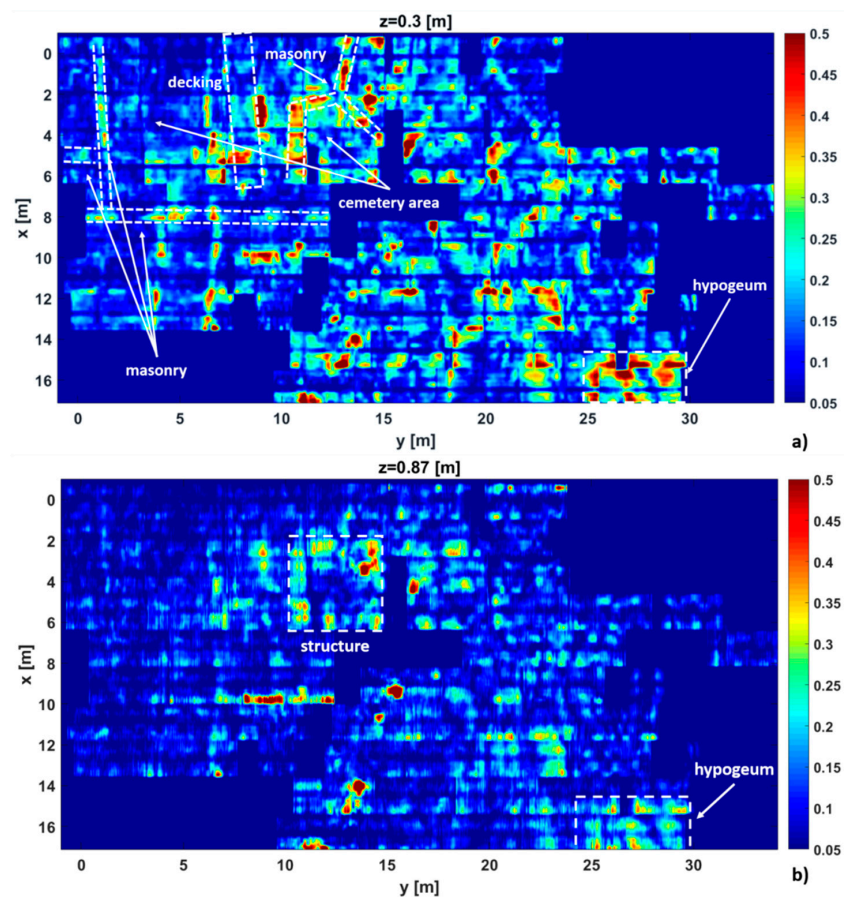


Figure 10. Interpretation of the pseudo-3D GPR tomographic results. Specifically, the images at the most significant depths are provided: (a) 0.3 m; (b) 0.87 m. The detected structures are represented by means of dashed white lines.

3.3. Villa dell'Unità d'Italia

Villa dell'Unità di Italia falls, from a lithological point of view, within an urban area affected by alluvial silt with the presence of coarser material; these alluvial deposits rest on the sub-Apennine clays which, in turn, are overlapped with calcarenite deposits (see Figure 11). The presence of the clay materials in the shallow subsurface suggested a plan of only the ERT investigations. In fact, the high conductivity of the clay layers ($\rho < 10 \Omega\text{m}$) strongly reduces the penetration depth of microwaves.

The ERT survey was carried out using a Syscal Pro Swich 96 with 96 electrodes regularly distributed on the surface. The measurements were carried out along three profiles selected to minimize the effect of the anthropic noise and to avoid the presence of the obstacles to install the electrode sensors. For each profile 2D ERT images were obtained using the ERT Lab software (Figure 11a). To have a spatial representation of the resistivity patterns, a pseudo-3D map was obtained with a simple interpolation (Figure 11b).

The analysis of the ERT images with the constraints of the geological field survey, highlights four main aspects:

- The presence of a 2–3-m thick shallow resistive layer (100–200 Ωm), that could be associated to filling material, locally affected by underground services;

- In all the ERTs, the occurrence of a very conductive layer ($2\text{--}3\ \Omega\text{m}$), probably related to alluvial silt deposits with remarkable water content;
- The existence at the bottom of a moderate resistivity layer ($2\text{--}25\ \Omega\text{m}$) correlated with the sub-Apennine clays;
- The identification, on the right of all the ERT images, of a sector with electrical resistivity values ranging in the interval $30\text{--}50\ \Omega\text{m}$ related to the calcarenite substratum in heteropic contact with the sub-Apennine clays, as reported in the geological map [30].

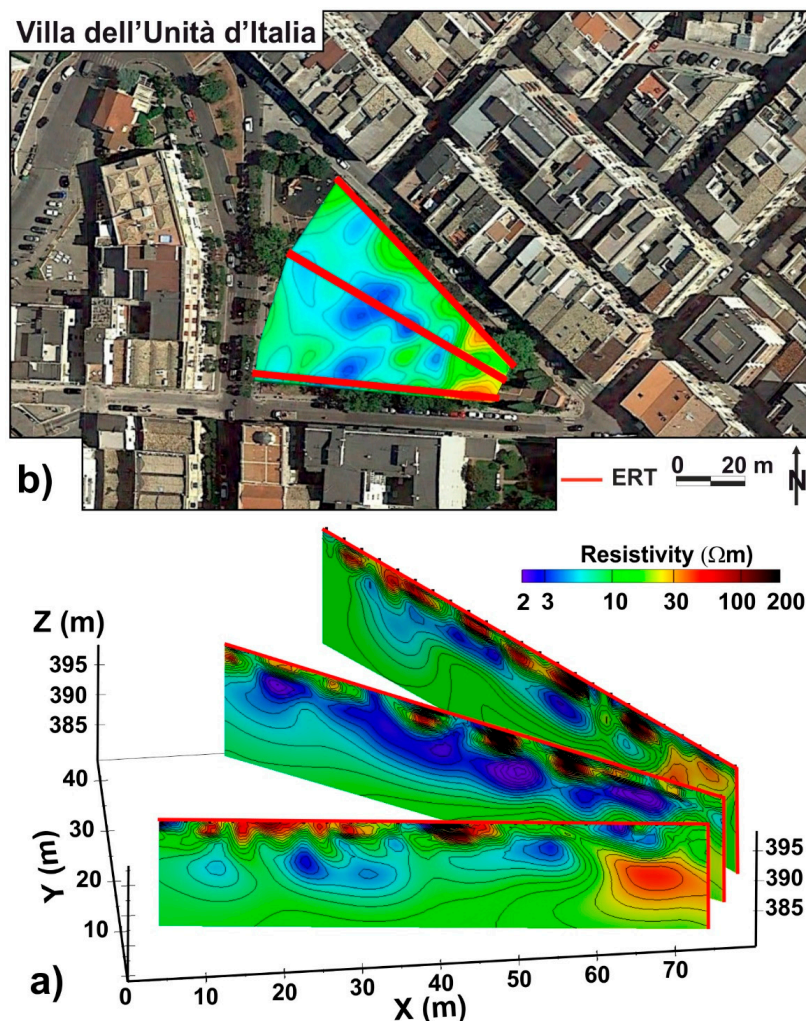


Figure 11. Results of the ERT investigation at Villa d'Unità di Italia. (a) 2D ERT images obtained along three different profiles are reported. (b) A map of the resistivity at depth = 10 m is displayed. The presence of a conductive zone associated to the presence of alluvial deposits with high water content and a sharp resistivity contrast on the right side of the square is quite evident. (Image modified from Google Earth).

4. Conclusions

Three test sites located in the urban area were selected: Piazza Duomo; Piazza San Giovanni and Villa d'Unità d'Italia. The complexity of the geological setting and the presence of large and diffuse anthropic structures in the near subsurface allowed us to have challenging and interesting test sites for the application of novel electrical and electromagnetic tomographic methods.

The interpretation of the results discloses the way to discuss the potentiality and the limitations of GPR and ERT methods as referred to the general context of urban geophysics. Indeed, the historical areas of Matera represents an ideal outdoor laboratory for testing the capacity of GPR and ERT

methods to illuminate and reconstruct the geometry of buried structures, being its urban subsurface a complex geological environment that was continuously modified by the anthropic activities during the millenarian history of the city.

The use of the tomographic approach for GPR data inversion was the key for obtaining a 3D geometrical reconstruction of the underground structures in a complex geological environment. The results obtained in Piazza Duomo are remarkable, where the geometry of a cistern for the water storage was fully reconstructed. At the same time, the ERT is a powerful method for exploring the near surface without any limitation about the depth of investigation, but with a spatial resolution lower than the GPR method. However, the application of the ERT method provides information even in the presence of extremely conductive layers, when the propagation of the GPR signals is strongly limited. The results of the geophysical survey carried out in the test site of Villa dell'Unità di Italia confirm the key role of the ERT method in exploring conductive underground environment.

To date, the joint application of GPR and ERT methods, the use of novel tomographic approaches for data inversion and ICT techniques for data visualization can be considered a powerful tool for obtaining 3D imaging of the subsurface in urban areas.

As it concerns future research directions, the combination of GPR and ERT methods with other non-invasive and cost-effective sensors (i.e., MEMS, Fiber Optics) and ICT tools for geospatial data sharing and visualization will play a key role in urban planning. This approach responds to the scientific challenges of urban geophysics by integrating the latest enabling technologies for the geophysical exploration of the subsurface.

Finally, the case-study of Matera represents an extraordinary “Living Lab” to transform historic centers into urban laboratories where researchers, technicians of innovative companies, technicians of public institutions and citizen associations (quadruple-helix model of innovation) can actively participate in developing new strategies for smart and resilient cities.

Author Contributions: Methodology, J.B., G.C., I.C., A.C., G.G., A.G., F.F., G.L., G.M., A.P., S.P.; investigation, J.B., G.C., I.C., A.C., G.G., A.G., F.F., G.L., G.M., A.P., S.P.; supervision F.S. and V.L.; Project administration, C.C.; Funding acquisition, C.C. All authors have read and agreed to the published version of the manuscript.

Funding: This work was supported by the Clara Project (SCN_00451) funded by MIUR (Smart Cities and Communities and Social Innovation Program, PON R&S 2007-2013).

Acknowledgments: We thank the administration of the Matera Municipality and Matera 2019 Foundation for their support to organize the geophysical surveys and to disseminate the scientific results of this activity.

Conflicts of Interest: The authors declare no conflicts of interest.

References

1. Meijer, A.; Bolivar, M. Governing the smart city: A review of the literature on smart urban governance. *Int. Rev. Adm. Sci.* **2016**, *82*, 392–408. [[CrossRef](#)]
2. Trindade, E.P.; Hinning, M.P.; Moreira da Costa, E.; Sabatini Marques, J.; Cid Bastos, R.; Yigitcanlar, T. Sustainable development of smart cities: A systematic review of the literature. *J. Open Innov. Technol. Mark. Complex.* **2017**, 3–11. [[CrossRef](#)]
3. Salvia, M.; Cornacchia, C.; Di Renzo, G.C.; Braccio, G.; Annunziato, M.; Colangelo, A.; Orifici, L.; Lapenna, V. Promoting smartness among local areas in a Southern Italian region: The Smart Basilicata Project. *Indoor Built Environ.* **2016**, *25*, 1024–1038. [[CrossRef](#)]
4. Desouza, K.C.; Flanery, T.H. Designing, planning, and managing resilient cities: A conceptual framework. *Cities* **2013**, *35*, 89–99. [[CrossRef](#)]
5. Arafah, Y.; Winarso, H. Redefining smart city concept with resilience approach. *IOP Conf. Ser. Earth Environ. Sci.* **2017**, *70*, 012065. [[CrossRef](#)]
6. Cuomo, V.; Soldovieri, F.; Ponzo, F.C.; Ditommaso, R. A holistic approach to long term SHM of transport infrastructures. In *The International Emergency Management Society (TIEMS) Newsletter*; THE International Emergency Management Society: Brussels, Belgium, 2018; pp. 67–84, ISSN 2033-1614.

7. Showstack, R. Scientist call for a renewed emphasis on urban geology. *EOS Earth Space Sci. News* **2014**, *47*, 431–432. [[CrossRef](#)]
8. Bobylev, N. Sterling, Urban underground space: A growing imperative perspectives and current research in planning and design for underground space use. *Tunn. Undergr. Space Technol.* **2016**, *55*, 1–4. [[CrossRef](#)]
9. Bobylev, N. Underground space as an urban indicator: Measuring use of subsurface. *Tunn. Undergr. Space Technol.* **2016**, *55*, 40–51. [[CrossRef](#)]
10. Lapenna, V. Resilient and sustainable cities of tomorrow: The role of applied geophysics. *Boll. Geofis. Teor. Appl.* **2017**, *58*, 237–251. [[CrossRef](#)]
11. Laureano, P. *Iscrizione alla Lista del Patrimonio Mondiale, Comune di Matera, I Sassi e il Parco delle Chiese Rupestri; Verso il Piano di Gestione del sito UNESCO: Matera, Italy*, 2012.
12. Tropeano, M.; Sabato, L.; Festa, V.; Capolongo, D.; Casciano, C.I.; Chiarella, D.; Gallicchio, S.; Longhitano, S.G.; Moretti, M.; Petruzzelli, M.; et al. “Sassi”, the old town of Matera (southern Italy): First aid for geotourists in the “European Capital of Culture 2019. *Alp. Mediterr. Quat.* **2018**, *31*, 133–145. [[CrossRef](#)]
13. Tropeano, M.; Sabato, L.; Pieri, P. Filling and cannibalization of a foredeep: The Bradanic Trough, Southern Italy. *Geol. Soc. Lond. Spec. Publ.* **2002**, *191*, 55–79. [[CrossRef](#)]
14. Beneduce, P.; Festa, V.; Francioso, R.; Schiattarella, M.; Tropeano, M. Conflicting drainage patterns in the Matera Horst area, Southern Italy. *Phys. Chem. Earth* **2004**, *29*, 717–724. [[CrossRef](#)]
15. Festa, V.; Sabato, L.; Tropeano, M. 1:5000 geological map of the upper Cretaceous intraplateau-basin succession in the “Gravina di Matera” canyon (Apulia Carbonate Platform, Basilicata, southern Italy). *Ital. J. Geosci.* **2018**, *137*, 3–15. [[CrossRef](#)]
16. Solimene, R.; Catapano, I.; Gennarelli, G.; Cuccaro, A.; Dell’Aversano, A.; Soldovieri, F. SAR Imaging Algorithms and some Unconventional Applications: A Unified Mathematical Overview. *IEEE Signal Proc. Mag.* **2014**, *31*, 90–98. [[CrossRef](#)]
17. Persico, R. *Introduction to Ground Penetrating Radar: Inverse Scattering and Data Processing*; John Wiley & Sons: Hoboken, NJ, USA, 2014.
18. Catapano, I.; Gennarelli, G.; Ludeno, G.; Soldovieri, F.; Persico, R. Ground-Penetrating Radar: Operation Principle and Data Processing. *Wiley Encycl. Electr. Electron. Eng.* **2019**, 1–23. [[CrossRef](#)]
19. Catapano, I.; Gennarelli, G.; Ludeno, G.; Soldovieri, F. Applying Ground-Penetrating Radar and Microwave Tomography Data Processing in Cultural Heritage: State of the art and future trends. *IEEE Signal Process. Mag.* **2019**, *36*, 53–61. [[CrossRef](#)]
20. Catapano, I.; Ludeno, G.; Soldovieri, F.; Tosti, F.; Padeletti, G. Structural Assessment via Ground Penetrating Radar at the Consoli Palace of Gubbio (Italy). *Remote Sens.* **2018**, *10*, 45. [[CrossRef](#)]
21. Bertero, M.; Boccacci, M. *Introduction to Inverse Problems in Imaging*; CRC Press: London, UK; Taylor&Francis Group: London, UK, 1998.
22. Giocoli, A.; Hailemichael, S.; Bellanova, J.; Calamita, G.; Perrone, A.; Piscitelli, S. Site and building characterization of the Orvieto Cathedral (Umbria, Central Italy) by electrical resistivity tomography and single-station ambient vibration measurements. *Eng. Geol.* **2019**, *260*, 105195. [[CrossRef](#)]
23. Moscatelli, M.; Piscitelli, S.; Piro, S.; Stigliano, F.; Giocoli, A.; Zamuner, D.; Marconi, F. Integrated geological and geophysical investigations to characterize the anthropic layer of the Palatine hill and Roman Forum (Rome, Italy). *Bull. Earthq. Eng.* **2014**, *12*, 1319–1338. [[CrossRef](#)]
24. Pazzi, V.; Tapete, D.; Cappuccini, L.; Fanti, R. An electric and electromagnetic geophysical approach for subsurface investigation of anthropogenic mounds in an urban environment. *Geomorphology* **2016**, *273*, 335–347. [[CrossRef](#)]
25. Rizzo, E.; Capozzoli, L.; De Martino, G.; Grimaldi, S. Urban geophysical approach to characterize the subsoil of the main square in San Benedetto del Tronto town (Italy). *Eng. Geol.* **2019**, *257*, 105–133. [[CrossRef](#)]
26. Morelli, G.; Labrecque, D.J. Advances in ERT inverse modeling. *Eur. J. Environ. Eng. Geophysics* **1996**, *1*, 171–186.
27. Novo, A.; Vinent, M.L.; Levy, T.M. Geophysical Surveys at Khirbat Faynan, an Ancient Mound Site in Southern Jordan. *Int. J. Geophys.* **2012**, *2012*, 8. [[CrossRef](#)]
28. Sogliani, F. Archeologia urbana a Matera. In *Dall’indagine Stratigrafica alla Condivisione dei Dati: Lo Scavo di S. Giovanni Battista-S. Maria La Nova. Mappa Data Book 1*; Edizioni Nuova Cultura: Roma, Italy, 2015.

29. Piscitelli, S.; Rizzo, E.; Cristallo, F.; Lapenna, V.; Crocco, L.; Persico, R.; Soldovieri, F. GPR and microwave tomography for detecting shallow cavities in the historical area of “Sassi of Matera” (Southern Italy). *Near Surface Geophys.* **2007**, *5*, 275–284. [[CrossRef](#)]
30. Studio Geologico RU Matera. Studio Geologico Tecnico. Carta Geologica Centro Capoluogo Parte Nord. 2014. Available online: <https://www.comune.matera.it/amministrazione-trasp/pianificazione-e-governo-del-territorio> (accessed on 13 January 2017).



© 2020 by the authors. Licensee MDPI, Basel, Switzerland. This article is an open access article distributed under the terms and conditions of the Creative Commons Attribution (CC BY) license (<http://creativecommons.org/licenses/by/4.0/>).